

The Structure of the Route to the Period-three Orbit in the Collatz Map

Weicheng Fu^{1,2,3*} and Yisen Wang^{3†}

¹ *Department of Physics, Tianshui Normal University,
Tianshui 741000, Gansu, China*

² *Key Laboratory of Atomic and Molecular Physics & Functional Material of Gansu Province,
College of Physics and Electronic Engineering,
Northwest Normal University, Lanzhou 730070, China*

³ *Lanzhou Center for Theoretical Physics,
Key Laboratory of Theoretical Physics of Gansu Province,
and Key Laboratory of Quantum Theory and Applications of MoE,
Lanzhou University, Lanzhou, Gansu 730000, China*

(Dated: February 11, 2025)

This study analyzes the Collatz map through nonlinear dynamics. By embedding integers in Sharkovsky’s ordering, we show that odd initial values suffice for full dynamical characterization. We introduce “direction phases” to partition iterations into upward and downward phases, and derive a recursive function family parameterized by upward phase counts. Consequently, a logarithmic scaling law between iteration steps and initial values is revealed, demonstrating finite-time convergence to the period-three orbit. Moreover, we establish the equivalence of the Collatz map to a binary shift map, whose ergodicity guarantees universal convergence to attractors, providing additional support for convergence. Furthermore, we identify that basins of attraction follow power-law distributions and find that odd numbers classified by upward phases follow Gamma statistics. These results offer valuable insights into the dynamics of discrete systems and their connections to number theory.

I. INTRODUCTION

Dynamic systems exhibiting behaviors from periodic oscillations to chaotic phenomena are ubiquitous in nature and engineering [1–6]. Nonlinear dynamics provides a systematic framework to analyze and predict the evolution of such complex systems [7]. Discrete dynamical systems, governed by difference equations and characterized by iterative state transitions, serve as effective models for phenomena including population dynamics, digital signal processing, and economic cycles [8]. These systems exhibit diverse behaviors such as periodicity, chaos, bifurcations, and fractal patterns [9–11], with their theoretical significance and practical relevance establishing them as a central focus in nonlinear dynamics research [12–19].

In nonlinear dynamics, Sharkovsky’s theorem [20, 21] and Li-Yorke’s theorem [22] are foundational results. Sharkovsky’s theorem establishes the coexistence of periodic solutions in one-dimensional discrete maps, known as Sharkovsky’s ordering [23], demonstrating that specific periodic solutions imply the existence of others. Notably, a period-three solution guarantees solutions for all integer periods. Li-Yorke’s theorem, encapsulated by “Period three implies chaos” [22], both recontextualizes Sharkovsky’s insight and rigorously defines chaos. It shows chaotic systems exhibit extreme sensitivity to initial conditions: infinitesimal differences in initial states diverge exponentially, precluding long-term predictabil-

ity [24, 25]. This discovery of deterministic chaos overturns classical assumptions that certainty ensures predictability. While Newtonian mechanics struggles with nonlinear systems, chaos theory redefines our understanding of complexity [26–28]. Importantly, the “Period three implies chaos” principle applies exclusively to continuous interval self-maps and does not generalize to discrete maps.

In this study, we analyze the Collatz map as a discrete dynamical system, employing methods from nonlinear dynamics to investigate its statistical behavior [29]. The Collatz map also known as the Collatz conjecture (or $3X+1$ problem), renowned for its simple formulation [30] and unresolved status [31–36], posits that iterating the transformation

$$X = \begin{cases} 3X + 1 & \text{if } X \text{ is odd,} \\ X/2 & \text{if } X \text{ is even,} \end{cases} \quad (1)$$

will eventually reduce any positive integer X to the cycle $\{4, 2, 1\}$.

Significant progress has been made in characterizing the probabilistic behavior of Collatz orbits. Foundational work by Crandall [37] established constraints linking the map to Diophantine equations, while subsequent studies like Krasikov’s statistical approximations [38] advanced a probabilistic framework. Recent advances by Tao [34] leverage random walks and skew distributions on cyclic groups to demonstrate convergence for “almost all” integers (in logarithmic density), offering strong heuristic support for the conjecture.

The Collatz conjecture hinges on two requirements: (i) proving *uniqueness* (i.e., that $\{4, 2, 1\}$ is the sole periodic

* fuweicheng@tsnu.edu.cn

† wys@lzu.edu.cn

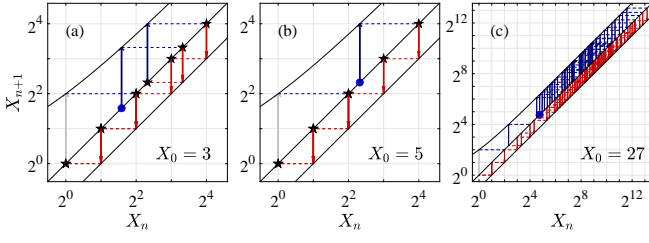


FIG. 1. A cobweb plot for orbits of different X_0 .

cycle), and (ii) demonstrating *convergence* (i.e., finite iterations terminating at this cycle). Fulfilling both would resolve the conjecture, yet despite computational verification for astronomically large integers, a universal proof remains beyond reach.

In this work, we employ Sharkovsky's ordering to represent integers and prove that analyzing Collatz map iterations necessitates focusing solely on odd initial values. By introducing “direction phases”—classifying iterations into upward and downward phases—we derive a recursive function family parameterized by upward-phase counts. This reveals a logarithmic relationship between iteration steps and initial values, demonstrating finite-time convergence to the period-three orbit $\{4, 2, 1\}$. Furthermore, we establish equivalence between the Collatz map and a binary shift map. The ergodicity of the shift map [39] ensures inevitable evolution toward attractors, reinforcing convergence. Numerical analysis shows that attraction basins obey power-law distributions, while odd numbers grouped by upward phases approximately follow Gamma distributions. However, directly proving the cycle's uniqueness remains unresolved, as discussed later. Our findings bridge discrete dynamics and number theory.

The paper is structured as follows: Section II defines the Collatz map and introduces the concept of “direction phases”, Section III develops the theoretical framework, Section IV validates results numerically, and Section V concludes with open challenges.

II. THE COLLATZ MAP AND DEFINITION OF DIRECTION PHASES

For brevity, the map (1) is abbreviated as

$$X_n = M(X_{n-1}) = M^n(X_0), \quad (2)$$

where $n, X_n \in \mathbb{Z}^+$. The Collatz conjecture asserts

$$\lim_{n \rightarrow \infty} M^n(X_0) = \{4, 2, 1\} \quad \text{for } \forall X_0 \in \mathbb{Z}^+, \quad (3)$$

i.e., all trajectories eventually enter the period-three orbit $\{4, 2, 1\}$.

To formalize the dynamics, we introduce “direction phases” [40]:

$$\begin{cases} P_{\uparrow}(n) = 1, & \text{if } X_{n+1} > X_n \quad (\text{up phase}); \\ P_{\downarrow}(n) = -1, & \text{if } X_{n+1} < X_n \quad (\text{down phase}). \end{cases} \quad (4)$$

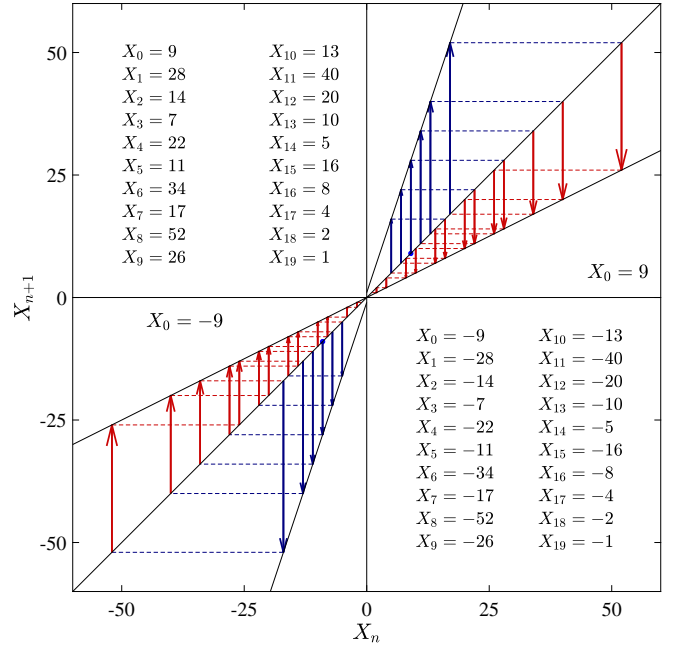


FIG. 2. A cobweb plot for orbits of $X_0 = \pm 9$. In the second and fourth quadrants give the values of iterative sequences for $X_0 = 9$ and $X_0 = -9$, respectively.

Let N_{\uparrow} and N_{\downarrow} denote the number of up and down phases *before* entering $\{1, 4, 2\}$, respectively. For example, Figs. 1(a)-(c) show trajectories for $X_0 = 3, 5, 27$, yielding $(N_{\uparrow}, N_{\downarrow}) = (2, 5), (1, 4), (41, 70)$, respectively.

Notably, N_{\uparrow} and N_{\downarrow} correspond to the counts of odd and even terms in the sequence from $X_0 \neq 1$ to 2. The total iterations satisfy

$$N = N_{\uparrow} + N_{\downarrow}, \quad \text{with } M^N(X_0) = 1. \quad (5)$$

The Collatz map generalizes to all integers via

$$X_{n+1} = \begin{cases} 3X_n + \text{sgn}(X_n) & (\text{odd } X_n), \\ X_n/2 & (\text{even } X_n), \end{cases} \quad (6)$$

where $X_n \in \mathbb{Z}$. The extended conjecture becomes

$$\lim_{n \rightarrow \infty} M^n(X_0) = \begin{cases} \{-1, -4, -2\} & X_0 \in \mathbb{Z}^-, \\ \{0\} & X_0 = 0, \\ \{4, 2, 1\} & X_0 \in \mathbb{Z}^+. \end{cases} \quad (7)$$

Figure 2 illustrates symmetric trajectories for $X_0 = \pm 9$, converging to ± 1 . This work focuses on $X_0 \in \mathbb{Z}^+$; subsequent sections detail the theoretical framework.

III. THEORETICAL ANALYSIS

We define two infinite-dimensional vectors:

$$\mathbf{B} = [2^0, 2^1, 2^2, \dots, 2^m, \dots], \quad (8)$$

$$\mathbf{O} = [3, 5, 7, \dots, 2n+1, \dots], \quad (9)$$

and the matrix $\mathbf{D} = \mathbf{B}^T \mathbf{O}$, explicitly structured as

$$\mathbf{D} = \begin{bmatrix} 3 \cdot 2^0 & 5 \cdot 2^0 & \dots & (2n+1) \cdot 2^0 & \dots \\ 3 \cdot 2^1 & 5 \cdot 2^1 & \dots & (2n+1) \cdot 2^1 & \dots \\ \vdots & \vdots & \ddots & \vdots & \vdots \\ 3 \cdot 2^m & 5 \cdot 2^m & \dots & (2n+1) \cdot 2^m & \dots \\ \vdots & \vdots & \ddots & \vdots & \vdots \end{bmatrix}. \quad (10)$$

Let \mathbb{B} , \mathbb{O} , and \mathbb{D} denote the sets formed by the elements of \mathbf{B} , \mathbf{O} , and \mathbf{D} , respectively. By Sharkovsky's ordering [20], $\mathbb{D} \cup \mathbb{B} \equiv \mathbb{Z}^+$.

It is clear that if $X_0 = 2^m \in \mathbb{B}$, then $M^m(X_0) = 1$ with $N_\uparrow = 0$ and $N = N_\downarrow = m$ (trivial trajectory); if $X_0 = (2n+1) \cdot 2^m \in \mathbb{D}$, then $M^m(X_0) = 2n+1 \in \mathbb{O}$. Thus, analyzing the Collatz map reduces to studying initial values $X_0 \in \mathbb{O}$.

A. Estimation of iteration steps

- *Case I:* $N_\uparrow = 1$.

For $X_0 \in \mathbb{O}$ with $N_\uparrow = 1$, we derive

$$X_0 = F_1(m) = \frac{2^m - 1}{3} \in \mathbb{O} \quad (m > 2). \quad (11)$$

It is easily to prove that $F_1(m) \in \mathbb{O}$ iff $m = 2p$, yielding

$$F_1(p) = \frac{4^p - 1}{3}, \quad p \geq 2, \quad (12)$$

with recursion

$$F_1(p) = 4^{p-1} + F_1(p-1). \quad (13)$$

The iteration steps for convergence is given by

$$N_1 = N_\downarrow + N_\uparrow = 1 + 2p = 1 + \log_2(3X_0 + 1). \quad (14)$$

Note that $F_1(1) \equiv 1 \in \mathbb{B}$ from Eq. (12).

- *Case II:* $N_\uparrow = 2$.

For $X_0 \in \mathbb{O}$ with $N_\uparrow = 2$, we have

$$X_0 = F_2(p, k_1) = \frac{2^{k_1} F_1(p) - 1}{3} \quad (k_1 \geq 1), \quad (15)$$

It is evident that

$$F_2(p, k_1) = F_2(p, k_1 - 2) + 2^{k_1-2} F_1(p), \quad (16)$$

and $k_1 = \log_2(3X_0 + 1) - \log_2(X_0)$. Thus, the iteration steps for convergence is

$$N_2 = 2 + 2p + k_1 = 2 + 2\log_2(3X_0 + 1) - \log_2(X_0). \quad (17)$$

- *General Case:* $N_\uparrow = s$.

For $X_0 \in \mathbb{O}$ with $N_\uparrow = s$, recursively define

$$X_0 = F_s(p, k_{s-1}) = \frac{2^{k_{s-1}} F_{s-1}(p, k_{s-2}) - 1}{3}, \quad (18)$$

with $k_{s-1} = \log_2(3X_0 + 1) - \log_2(X_0) \in \mathbb{Z}^+$. The function F_s follows the recursion relation

$$F_s(p, k_{s-1}) = F_s(p, k_{s-1} - 2) + 2^{k_{s-1}-2} F_{s-1}(p, k_{s-2}). \quad (19)$$

Total iterations follow

$$\begin{aligned} N_s &= N_\uparrow + N_\downarrow = s + 2p + \sum_{j=1}^{s-1} k_j \\ &= s + s \log_2(3X_0 + 1) - (s-1) \log_2(X_0) \\ &= s [1 + \log_2(3 + 1/X_0)] + \log_2(X_0), \end{aligned} \quad (20)$$

implying logarithmic growth of N_s with X_0 .

Actually, the function F_s can be expressed in an explicit form. For example, F_4 can be written as

$$\begin{aligned} F_4(p, k_3) &= \frac{2^{k_3} \left\{ \frac{2^{k_2} \left[\frac{2^{k_1} \left(\frac{4^p - 1}{3} \right) - 1}{3} \right] - 1}{3} \right\} - 1}{3} = \\ &= \frac{2^{2p+k_1+k_2+k_3}}{3^4} - \frac{2^{k_1+k_2+k_3}}{3^4} - \frac{2^{k_2+k_3}}{3^3} - \frac{2^{k_3}}{3^2} - \frac{1}{3}. \end{aligned} \quad (21)$$

The function F_s can be further abbreviated as

$$F_s = \mathbf{a}_s \cdot \mathbf{b}_s, \quad (22)$$

where $\mathbf{a}_s \cdot \mathbf{b}_s$ denotes the inner product, and

$$\begin{aligned} \mathbf{a}_s &= \frac{1}{3^s} [1, -3^0, -3^1, \dots, -3^{s-3}, -3^{s-2}, -3^{s-1}], \\ \mathbf{b}_s &= [2^{k_s}, 2^{k_{s-1}}, 2^{k_{s-2}}, \dots, 2^{k_2}, 2^{k_1}, 2^0], \end{aligned} \quad (23)$$

with $k_s > k_{s-1} > k_{s-2} > \dots > k_1 \geq 1$. A similar function was presented in Ref. [30]. Note that if $X_0 = F_s$, then $N_\downarrow = k_s$, resulting in $N_s = s + k_s$.

In fact, the behavior of N_s/X_0 is more important than the specific magnitude of N_s . For instance, for $X_0 = 2^m \in \mathbb{B}$ and $m \rightarrow \infty$, we have $N_0 = m \rightarrow \infty$. However, we can also observe that

$$\lim_{m \rightarrow \infty} \frac{N_0}{X_0} = \lim_{m \rightarrow \infty} \frac{m}{2^m} = 0, \quad (24)$$

implying *finite* iterations for convergence.

For a give s , Eq. (20) leads to

$$\lim_{X_0 \rightarrow \infty} \frac{N_s}{X_0} = \lim_{X_0 \rightarrow \infty} \frac{1}{X_0 \ln 2} = 0, \quad (25)$$

validating convergence for $X_0 \in \mathbb{F}$, that is, the Collatz conjecture holds for $X_0 \in \mathbb{F}$, where \mathbb{F} is the set of all integers generated by the family of functions F_s . Equation (24) and (25) provide *proof of convergence*, aligning with Tao's probabilistic result [34].

Above analysis shows that if $\mathbb{F} \equiv \mathbb{O} \cup \{1\}$, that is, *if all odd numbers can be generated by F_s , the Collatz conjecture holds universally*. Proving this equivalence would indirectly establish uniqueness of the cycle $\{4, 2, 1\}$. However, providing a direct proof of this point is difficult, and efforts will continue in the future.

TABLE I. Statistics of numbers in different attraction basins p within a given range of $X_0 \in [3, 5, \dots, 2L + 1]$.

p	$L = 10^1$	10^2	10^3	10^4	10^5	10^6	10^7	10^8	10^9	10^{10}	10^{11}
2	9	94	940	9395	93679	938003	9378361	93772537	937676531	9377184597	93774780663
<u>3</u>	1	1	1	1	1	1	1	1	1	1	1
4	0	3	23	255	2412	23743	237828	2373777	23761165	237454856	2373306190
5	0	2	35	343	3842	37687	377838	3793838	37961580	379374692	3792124780
<u>6</u>	0	0	1	1	1	1	1	1	1	1	1
7	0	0	0	2	13	78	830	8098	80062	796409	7937609
8	0	0	0	3	50	448	4810	48229	485728	4843192	48398337
<u>9</u>	0	0	0	0	1	1	1	1	1	1	1
10	0	0	0	0	1	36	311	3253	32329	320937	3199254
11	0	0	0	0	0	2	15	212	2127	20883	206700
<u>12</u>	0	0	0	0	0	0	1	1	1	1	1
13	0	0	0	0	0	0	3	44	363	3419	34128
14	0	0	0	0	0	0	0	8	108	974	9551
<u>15</u>	0	0	0	0	0	0	0	0	1	1	1
16	0	0	0	0	0	0	0	0	2	12	88
17	0	0	0	0	0	0	0	0	0	7	78
<u>18</u>	0	0	0	0	0	0	0	0	0	0	1
19	0	0	0	0	0	0	0	0	0	0	4

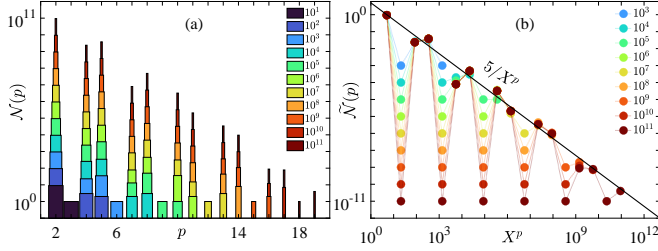


FIG. 5. (a) Histograms of number $\mathcal{N}(p)$ in different attraction basins p within a given range of $X_0 \in \{3, 5, \dots, 2L + 1\}$. The legend shows the value of L . (b) Same as the panel (a) but in normalized form $\tilde{\mathcal{N}}(p) = \mathcal{N}(p)/L$ and the horizontal axis is replaced by $X^p = F_1(p)$. The solid line serves as reference.

lar matrix. Of course, to observe non-zero values for larger p , a larger L is required. Based on the data, it is conjectured that as $p \rightarrow \infty$ and $L \rightarrow \infty$, then $\tilde{\mathcal{N}}(2) \approx 93.77\%$, $\tilde{\mathcal{N}}(4) \approx 2.37\%$, and $\tilde{\mathcal{N}}(5) \approx 3.79\%$, that is, $\tilde{\mathcal{N}}(2) + \tilde{\mathcal{N}}(4) + \tilde{\mathcal{N}}(5) \approx 99.93\%$ remains essentially unchanged, and increasing p and L only affects the significant digits of the decimal point. It is clear that *the size of basin of attraction follows a power-law distribution*.

Figure 6(a) displays the ratio $N_{\downarrow}/N_{\uparrow}$ as a function of X_0 . Different colored points represent numbers belonging to different basins of attraction. The solid lines correspond to theoretical predictions given by Eq. (20). It is seen that the theoretical and numerical results align very well. Additionally, the ratio approaches $\log_2(3) \approx 1.585$ as N_{\uparrow} increases, as indicated by the purple horizontal dashed line. Figure 6(b) shows the dependence of the total number of iterations, N , on X_0 . Note that N grows slowly as X_0 increases. The numerical results are fully consistent with the theoretical predictions, as shown by

the solid lines from Eq. (20). This supports the conclusion that the number of iterations required for convergence is indeed a finite value relative to X_0 , confirming Eqs. (24) and (25). Furthermore, in Fig. 6(b), the purple crossed-dotted line marks the upper boundary of the region, which consists of the points with the smallest X_0 for a given N_{\uparrow} . We observe that the boundaries of the basins of attraction for different p resemble coastlines and exhibit a high degree of similarity. Notably, the distribution of the basin of attraction for $p = 2$ nearly covers the entire range of the calculated interval, which is consistent with the statistical results presented in Fig. 5. Specifically, the numbers on the upper boundary all belong to the basin of attraction of $p = 2$.

To investigate the properties of the numbers at the upper boundary marked in Fig. 6(b) in more detail, we present the behavior of these numbers over a broader range in Fig. 7. The abscissa (X_0) and ordinate (N) of the boundary points in Fig. 6(b) as functions of N_{\uparrow} are shown in Figs. 7(a)-(c). Figure 7(a) demonstrates that X_0 increases nearly in a stretched exponential manner with N_{\uparrow} (see the magenta dashed curve), which is faster than a power-law growth (black dashed line), but slower than exponential growth (black dashed line in the inset). Figure 7(b) provides a clearer depiction of how X_0 increases with N_{\uparrow} , i.e., $X_0 \propto \exp(1.2N_{\uparrow}^{1/2})$. Additionally, a self-similarity fractal structure, reminiscent of a coastline, is observed in the distribution of X_0 .

Figure 7(c) shows the dependence of N on N_{\uparrow} , where N increases approximately linearly with N_{\uparrow} . From Eq. (20), for a large X_0 , we have $N \approx [1 + \log_2(3)]N_{\uparrow}$, which agrees with the numerical results very well. Figure 7(d) displays the ratio N/X_0 as a function of X_0 , where the black line represents the theoretical prediction derived from Eq. (20). It is clear that as $X_0 \rightarrow \infty$, $N/X_0 \rightarrow 0$,

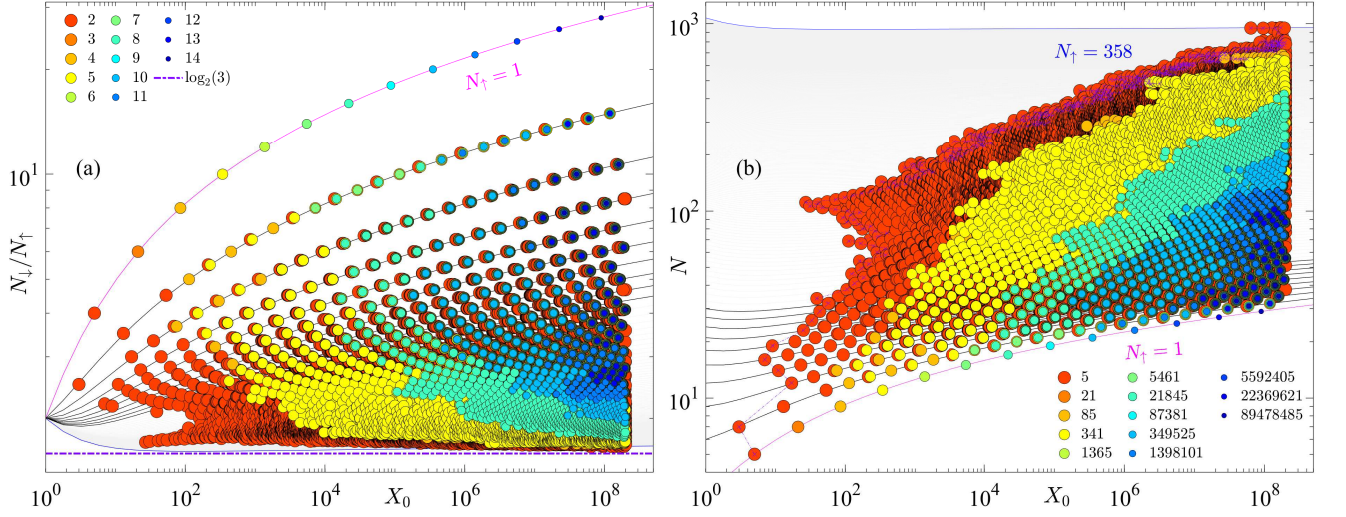


FIG. 6. The dependence of N_d/N_\uparrow (a) and $N = N_d + N_\uparrow$ (b) on $X_0 = 2n + 1$ for $n = 1, 2, \dots, 10^8$. Different colored points indicate belonging to different attraction basins p , see the legend in panel (a), while the legend in panel (b) shows the value of $F_1(p)$. The solid lines are the theoretical predictions given by expression (20). The dotted purple line marked by cross in panel (b) gives the upper boundary of the region, which is replotted in Fig. 7(a).

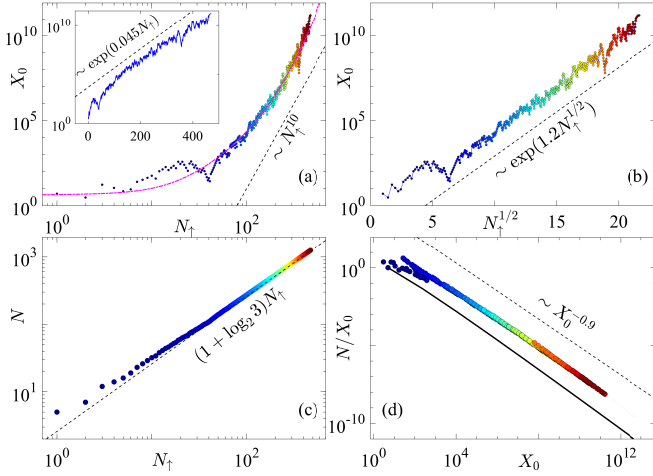


FIG. 7. (a) X_0 of the upper boundary points in Fig. 6(b) as a function of N_\uparrow in log-log scale. The magenta dashed line is a plot of a stretched exponential $\exp(1.2N_\uparrow^{1/2})/7 + 4$ for reference. Inset: Same as the main panel but in semi-log scale. (b) Same as the panel (a) but the abscissa is rescaled as $N_\uparrow^{1/2}$. The data in panels (c) and (d) are the same as that in panel (a) but shows in different forms. (c) $N = N_\uparrow + N_d$ as a function of N_\uparrow . (d) The dependence of N_\uparrow/X_0 on X_0 . The black line is given by formula (20) for $N_\uparrow = 1$. The dashed lines in all panels are plotted for reference.

indicating that the number of iterations required to converge to the period-three orbit becomes negligible relative to large X_0 . In this sense, the Collatz conjecture holds for all positive integers.

Figure 8 shows the distribution of numbers over N_\uparrow for a given range of $X_0 \in [3, 5, \dots, 2L + 1]$. In other words, the height of the histogram represents the pro-

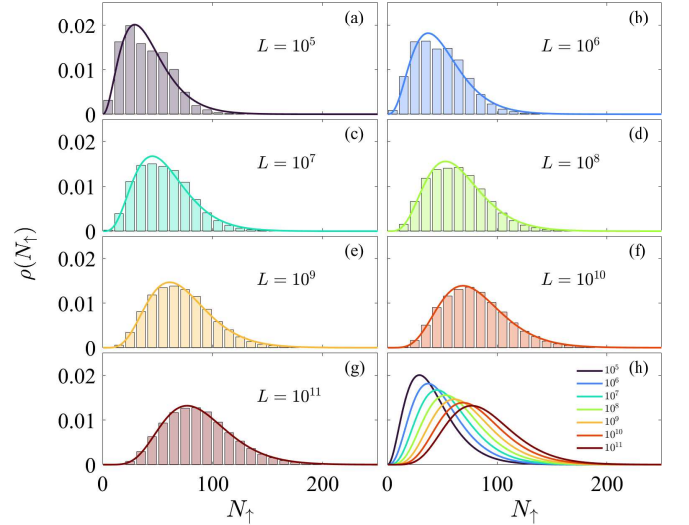


FIG. 8. (a)-(g) The distribution of numbers over N_\uparrow within a given interval of $X_0 \in [3, 5, \dots, 2L + 1]$. The solid line is a fitting curve based on the Gamma distribution with the form of $\rho(x) = \frac{A}{\Gamma(K)\theta^K} x^{K-1} e^{-x/\theta}$. (h) Summarize all fitted curves together for comparison.

portion of numbers with the same N_\uparrow . From Figs. 8(a)-(g), we observe that the distribution approximately follows a Gamma distribution with the form $\rho(x) = \frac{A}{\Gamma(K)\theta^K} x^{K-1} e^{-x/\theta}$ (see the solid line in each panel). Moreover, the distribution function becomes flatter as L increases, as shown by the solid lines in Fig. 8(h).

Figure 9(a) shows the dependence of the parameters of the Gamma distribution function on L . We observe that $A \simeq 1$ remains constant; K increases as L increases, concretely, $K \propto \log_{10}(L)$; and θ exhibits a slow decay,

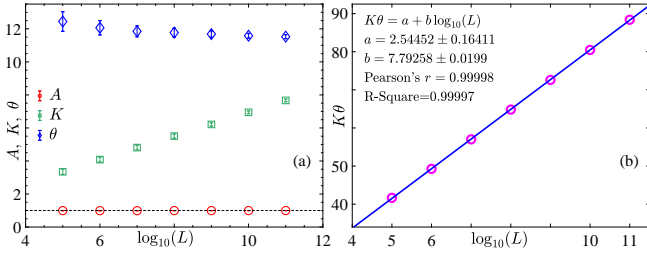


FIG. 9. (a) The fitting parameters of the Gamma distribution function in Fig. 8 as a function of L . (b) Dependence of the mean value of the Gamma distribution $K\theta$ on L .

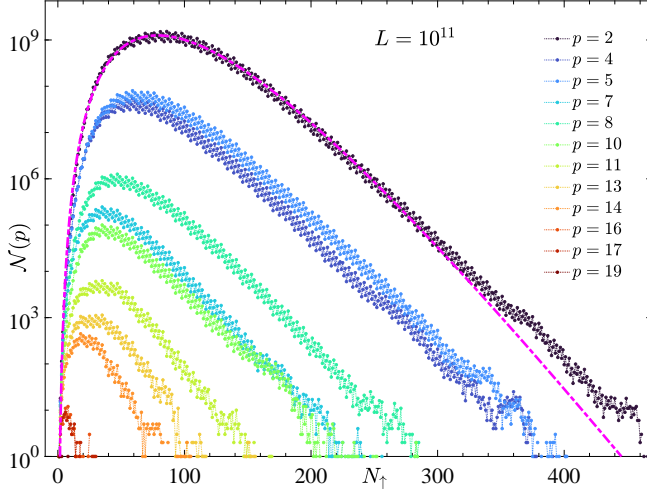


FIG. 10. The count number $\mathcal{N}(p)$ over N_+ within a given interval of $X_0 \in [3, 5, \dots, 2L + 1]$ in a semi-log scale. The magenta dashed line is a fitting curve based on the Gamma distribution.

remaining approximately constant within the range studied. As is known, the mean value of the Gamma distribution is given by $K\theta$, which also increases as L increases, as shown in Fig. 9(b). The best linear fitting suggests that the mean value of $\overline{N_+} = K\theta \approx 2.54 + 7.79 \log_{10}(L)$.

We further count the distribution of numbers in different basins of attraction over N_+ within the range $X_0 \in [3, 5, \dots, 2L + 1]$, where $L = 10^{11}$ is fixed (we have verified that changing the value of L produces qualitatively identical results). The numerical results are shown in Fig. 10, where $\mathcal{N}(p)$ represents the number of numbers belonging to the basin of attraction of p . It is evident that each $\mathcal{N}(p)$ follows a Gamma distribution, with different parameters for each p (see the magenta dashed curve, which nearly covers all points for $p = 2$).

V. SUMMARY AND DISCUSSIONS

In summary, we have investigated the Collatz map from the perspective of nonlinear dynamics, yielding four principal advances: First, by organizing positive integers via Sharkovsky's ordering, we demonstrate that analyzing odd initial values alone suffices to characterize Collatz dynamics. Second, we establish a classification system using "direction phases" to distinguish ascending and descending iteration patterns. This framework reveals a logarithmic scaling law between iteration steps and initial values through derived recursive functions F_s (parameterized by upward phase count s), proving finite-time convergence to the period-three cycle. Third, we identify dynamical equivalence between the Collatz map and a binary shift map, whose ergodicity guarantees universal convergence to attractors. Fourth, extensive numerical simulations show power-law distributed attraction basins and Gamma-distributed odd numbers across upward phases. These results offer valuable insights into the dynamics of discrete systems and their connections to number theory.

Furthermore, our analysis indicates that proving all odd numbers (> 1) are generated by the F_s function family would confirm the Collatz conjecture as a theorem. Within our computational range, all tested odd numbers align with F_s generation, supporting the conjecture that every odd number can be expressed in F_s 's form. However, a general proof of F_s 's universal generative capacity remains challenging and requires further investigation. Notably, studying F_s 's properties may provide novel perspectives on prime number distributions, given that all primes (except 2) belong to the odd number set theoretically covered by F_s .

ACKNOWLEDGMENTS

This work was supported by the National Science Foundation of China (Grants No. 12465010, No. 12247106, No. 12005156, No. 11975190, and No. 12247101). W. Fu also acknowledges support from the Youth Talent (Team) Project of Gansu Province, the Long-yuan Youth Talents Project of Gansu Province, the Fei-tian Scholars Project of Gansu Province, the Leading Talent Project of Tianshui City, the Innovation Fund from the Department of Education of Gansu Province (Grant No. 2023A-106), and the Open Project Program of Key Laboratory of Atomic and Molecular Physics & Functional Material of Gansu Province (6016-202404).

-
- [1] E. Ott, Strange attractors and chaotic motions of dynamical systems, *Rev. Mod. Phys.* **53**, 655 (1981).
 [2] J. J. Kozak, M. K. Musho, and M. D. Hatlee, Chaos, periodic chaos, and the random-walk problem, *Phys. Rev.*

- Lett.* **49**, 1801 (1982).
 [3] F. Mogavero, N. H. Hoang, and J. Laskar, Timescales of chaos in the inner solar system: Lyapunov spectrum and quasi-integrals of motion, *Phys. Rev. X* **13**, 021018

- (2023).
- [4] D. Pazó, Discontinuous transition to chaos in a canonical random neural network, *Phys. Rev. E* **110**, 014201 (2024).
 - [5] S.-D. Börner, C. Berke, D. P. DiVincenzo, S. Trebst, and A. Altland, Classical chaos in quantum computers, *Phys. Rev. Res.* **6**, 033128 (2024).
 - [6] D. Lippolis, Thermodynamics of chaotic relaxation processes, *Phys. Rev. E* **110**, 024215 (2024).
 - [7] A. Fuchs, *Nonlinear dynamics in complex systems* (Springer, 2014).
 - [8] R. H. Abraham, L. Gardini, and C. Mira, *Chaos in Discrete Dynamical Systems*, 1st ed. (Springer New York, NY, 1997).
 - [9] H.-O. Peitgen, H. Jürgens, and D. Saupe, *Chaos and Fractals: New Frontiers of Science*, 2nd ed. (Springer, 2004).
 - [10] K. E. Yao and Y. Shi, Hopf bifurcation in three-dimensional based on chaos entanglement function, *Chaos, Solitons & Fractals: X* **4**, 100027 (2019).
 - [11] H. Rouah, Stability analysis and suppress chaos in the generalized lorenz model, *Chaos, Solitons & Fractals: X* **12**, 100104 (2024).
 - [12] M. J. Feigenbaum, Quantitative universality for a class of nonlinear transformations, *J. Stat. Phys.* **19**, 25 (1978).
 - [13] B. V. Chirikov, A universal instability of many-dimensional oscillator systems, *Phys. Rep.* **52**, 263 (1979).
 - [14] E. Ott, *Chaos in Dynamical Systems*, 2nd ed. (Cambridge university press, 2002).
 - [15] M. C. Mackey, The dynamic origin of increasing entropy, *Rev. Mod. Phys.* **61**, 981 (1989).
 - [16] D. J. Driebe, *Fully Chaotic Maps and Broken Time Symmetry*, Nonlinear Phenomena and Complex Systems, Vol. 4 (Springer Dordrecht, 1999).
 - [17] C. Li, K. Tan, B. Feng, and J. Lü, The graph structure of the generalized discrete Arnold’s cat map, *IEEE Trans. Comput.* **71**, 364 (2022).
 - [18] J. A. Oliveira and F. E. Brochero Martínez, Dynamics of polynomial maps over finite fields, *Des. Codes Cryptogr.* **92**, 1113 (2024).
 - [19] C. Li, X. Lu, K. Tan, and G. Chen, Graph structure of chebyshev permutation polynomials over ring \mathbb{Z}_p^k , *IEEE Trans. Inf. Theory* **71**, 1419 (2025).
 - [20] A. N. Sharkovskii, Co-existence of the cycles of a continuous mapping of the line into itself, *Ukrain. Mat. Z.* **16**, 61 (1964).
 - [21] P. Štefan, A theorem of šarkovskii on the existence of periodic orbits of continuous endomorphisms of the real line, *Commun. Math. Phys.* **54**, 237 (1977).
 - [22] T.-Y. Li and J. A. Yorke, Period three implies chaos, *Amer. Math. Monthly* **82**, 985 (1975).
 - [23] P. E. Kloeden, On sharkovsky’s cycle coexistence ordering, *Bull. Aust. Math. Soc.* **20**, 171 (1979).
 - [24] C. Oestreicher, A history of chaos theory, *Dialogues Clin. Neuro.* **9**, 279 (2007).
 - [25] E. N. Lorenz, Deterministic nonperiodic flow, *J. Atmos. Sci.* **20**, 130 (1963).
 - [26] I. Prigogine and I. Stengers, *The end of certainty* (Simon and Schuster, 1997).
 - [27] G. M. Zaslavsky, *Hamiltonian chaos and fractional dynamics* (Oxford University Press, USA, 2005).
 - [28] J. Gleick, *Chaos: Making a New Science* (Penguin, 2008).
 - [29] Y. G. Sinai, Statistical $(3x + 1)$ problem, *Commun. Pure Appl. Math.* **56**, 1016 (2003).
 - [30] G. J. Wirsching, *The Dynamical System Generated by the $3n+1$ Function*, 1st ed., Lecture Notes in Mathematics, Vol. 1681 (Springer Berlin, Heidelberg, 1998).
 - [31] J. C. Lagarias, *The $3x+1$ problem: An annotated bibliography (1963–1999) (sorted by author)* (2011), [arXiv:math/0309224 \[math.NT\]](#).
 - [32] J. C. Lagarias, *The $3x+1$ problem: An annotated bibliography, ii (2000–2009)* (2012), [arXiv:math/0608208 \[math.NT\]](#).
 - [33] J. C. Lagarias, *The $3x+1$ problem: An overview* (2021), [arXiv:2111.02635 \[math.NT\]](#).
 - [34] T. Tao, Almost all orbits of the collatz map attain almost bounded values (2022), [arXiv:1909.03562 \[math.PR\]](#).
 - [35] Z. Hu, The analysis of convergence for the $3x + 1$ problem and crandall conjecture for the $ax + 1$ problem, *Advances in Pure Mathematics* **11**, 400 (2021).
 - [36] M. Wang, Y. Yang, Z. He, and M. Wang, The proof of the $3x + 1$ conjecture, *Advances in Pure Mathematics* **12**, 10 (2022).
 - [37] R. E. Crandall, On the “ $3x + 1$ ” problem, *Math. Comput.* **32**, 1281 (1978).
 - [38] I. Krasikov, How many numbers satisfy the $3x + 1$ conjecture?, *Internat. J. Math. & Math. Sci.* **12**, 791 (1989).
 - [39] M. Einsiedler and T. Ward, *Ergodic Theory: with a view towards Number Theory*, 1st ed., Graduate Texts in Mathematics, Vol. 259 (Springer London, 2011).
 - [40] W. Wang, Z. Liu, and B. Hu, Phase order in chaotic maps and in coupled map lattices, *Phys. Rev. Lett.* **84**, 2610 (2000).